

Sentence Curve Language Models

DongNyeong Heo¹ Heeyoul Choi¹

Abstract

Language models (LMs) are a central component of modern AI systems, and diffusion-based language models (DLMs) have recently emerged as a competitive alternative. Both paradigms rely on word embeddings not only to represent the input sentence, but also—implicitly—to represent the target sentence that backbone models are trained to predict. We argue that such static embedding of the target word is insensitive to neighboring words, encouraging locally accurate word prediction while neglecting global structure across the target sentence. To address this limitation, we propose a continuous sentence representation, termed **sentence curve**, defined as a spline curve whose control points affect multiple words in the sentence. Based on this representation, we introduce **sentence curve language model** (SCLM), which extends DLMs to predict sentence curves instead of the static word embeddings. We theoretically show that sentence curve prediction induces a regularization effect that promotes global structure modeling, and characterize how different sentence curve types affect this behavior. Empirically, SCLM achieves state-of-the-art performance among DLMs on IWSLT14 and WMT14, shows stable training without burdensome knowledge distillation, and demonstrates promising potential compared to discrete DLMs on LM1B.

1. Introduction

Language models (LMs) have demonstrated remarkable impact in real-world applications (Gemini et al., 2023; Achiam et al., 2023). Recently, diffusion language models (DLMs) (Sahoo et al., 2024; Nie et al., 2025) have attracted increasing attention due to their distinctive advantages, such as iterative refinement, bidirectional context awareness, and

¹Department of Computer Science and Electrical Engineering, Handong Global University, Pohang, South Korea. Correspondence to: DongNyeong Heo <sjglks@gmail.com>, Heeyoul Choi <hchoi@handong.edu>.

Preprint. February 3, 2026.

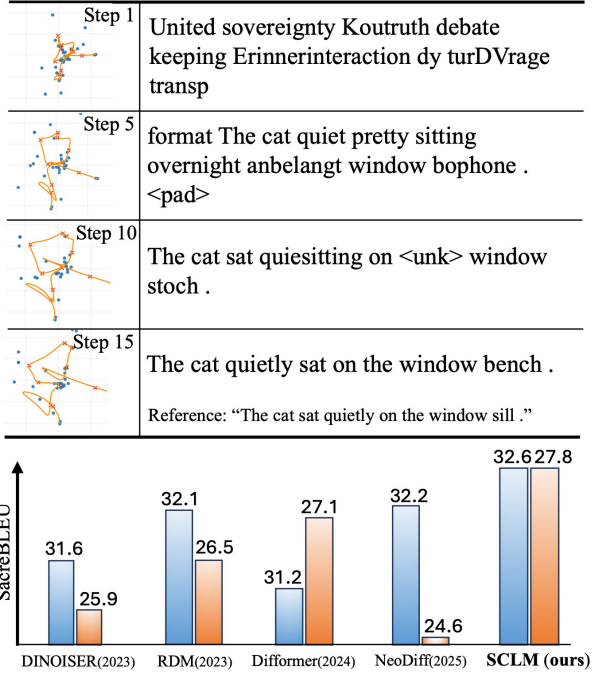


Figure 1. (Top) Sentence curve generation example of our SCLM in the denoising steps. More examples are illustrated in Figure 9 in Appendix C.3. (Bottom) Performance history of DLMs in IWSLT14 De→En (blue) and WMT14 En→De (orange).

fine-grained controllability. A fundamental component of both LMs and DLMs is the word embedding (Mikolov et al., 2013), which provides a distributed representation of individual words. A sentence is therefore represented as a sequence of word embeddings. Importantly, not only the input sentence but also the target sentence, which the model is enforced to predict, can be viewed as a sequence of word embeddings; we provide a detailed justification of this perspective in Section 3.

Although word embeddings can encode rich lexical information, they remain static with respect to neighboring words within a sentence. Using such embeddings as target representations therefore forces the model to predict a sequence of context-independent vectors. We argue that this static target representation can cause models to overfit to word-level local structure while neglecting sentence-level global structure. This issue can become particularly strengthened when input representations are noisy or imperfect, as in

non-autoregressive (non-AR) decoding and DLMs, where it can lead to practical problems such as the multimodality problem (Gu et al., 2017; Feng et al., 2025). Despite extensive research on input representations, the representation of target sentences has received comparatively little attention.

In the time-series modeling, (Hug et al., 2020) proposed modeling discrete time-series data using continuous spline curves, training neural networks to predict the curve rather than individual data points. Motivated by the work and the fact that a sentence is likely a sequence of symbolic elements, we propose *sentence curve*, a spline curve that traverses the word embeddings in vector space. Because the shape of sentence curve changes coherently with constituent words in the sentence, it can capture sentence-level global structure. Building on non-AR and semi-AR decoding models, such as DLMs, we introduce *sentence curve language model* (SCLM), which predicts target sentence curves instead of conventional static word embeddings (a sentence curve generation example is shown at the top of Figure 1). We further provide theoretical evidence that sentence curve prediction encourages models to focus more on global structure compared to the conventional approach. Furthermore, we develop a framework that clarifies how different sentence curve shapes affect the strength of the global structure regularization.

Through extensive experiments, we demonstrate that our proposed SCLMs achieve state-of-the-art (SOTA) performance among diffusion language models on neural machine translation (NMT) benchmarks, including IWSLT14 (Cettolo et al., 2014) and WMT14 (Bojar et al., 2014) (see the bottom of Figure 1), and even match the performance of AR Transformers (Vaswani et al., 2017) on a task. We further show that SCLMs can be trained stably without sequence-level knowledge distillation (KD) (Kim & Rush, 2016), which typically requires a burdensome pre-trained AR teacher. In addition, we explore the potential of SCLM for language modeling on LM1B (Chelba et al., 2013), where it exhibits advantageous training tendency than masked DLM (MDLM) (Sahoo et al., 2024). Lastly, empirical analyses on semi-AR language modeling reveal that SCLMs effectively enhance sentence-level global structure modeling. Together, we argue that these theoretical and empirical results suggest sentence curves as a promising direction for future non-AR and semi-AR models.

Our contributions can be summarized as follows:

- **Sentence Curve-based Target Reformulation:** We propose sentence curves, a continuous curve-based representation of sentences, and introduce them as an alternative target of sentence.
- **Sentence curve language model:** We incorporate sentence curve prediction into non-AR and semi-AR mod-

els, including DLMs, and demonstrate consistent improvements over prior DLMs on NMT and language modeling benchmarks.

- **Theoretic Framework for Global Structure Regularization:** We develop a framework that explains how sentence curve prediction induces sentence-level global structure regularization.
- **Empirical Validation:** Through extensive experiments and analyses, we provide empirical evidences supporting our theoretical insights.

2. Backgrounds

2.1. Notational Preliminaries

Throughout this paper, we frequently consider words and their corresponding embedding vectors (Mikolov et al., 2013). A word $y \in \mathcal{V}$ is a categorical variable, where \mathcal{V} denotes the vocabulary set. The embedding vector associated with a word is expressed as $\mathbf{e}_y = E\delta_y \in \mathbb{R}^d$, where δ_y is a one-hot vector with a single 1 element at position y , d is the embedding dimension, and $E = [\mathbf{e}_1, \dots, \mathbf{e}_{|\mathcal{V}|}] \in \mathbb{R}^{d \times |\mathcal{V}|}$ is the embedding matrix. A sentence of length L can then be represented as $Y = (y_1, \dots, y_L)$, or equivalently as $E_Y = [\mathbf{e}_{y_1}, \dots, \mathbf{e}_{y_L}]$ after embedding. We also frequently use probability measures, such as the model likelihood $p_\theta(Y)$, where θ denotes the model parameters. The true data likelihood is denoted by $p_{data}(Y)$. For conditional text generation tasks, such as NMT, where a conditional sentence X is given, the corresponding likelihoods are expressed as $p_\theta(Y|X)$ and $p_{data}(Y|X)$.

2.2. Non-Autoregressive Models

In contrast to AR models, which factorize sentence probabilities autoregressively as $p(Y|X) = \prod_{i=1}^L p(y_i|y_{<i}, X)$, non-AR models (Gu et al., 2017) assume conditional independence among target words, $p(Y|X) = \prod_{i=1}^L p(y_i|X)$, enabling parallel generation and substantial speedups. However, non-AR models typically underperform compared to their AR counterparts. A primary cause is the multimodality problem (Gu et al., 2017), which arises from the independence assumption: without explicitly modeling dependencies among target words, predictions may originate from different modes of the target distribution. This issue becomes particularly severe when a single input can correspond to multiple valid target sentences (Huang et al., 2022).

To mitigate the problem, prior work has proposed techniques such as iterative refinement (Lee et al., 2018), sequence-level KD (Kim & Rush, 2016), and latent variable modeling (Shu et al., 2020; Heo & Choi, 2023). Despite these efforts, training non-AR models generally remains less stable than training AR models. DLMs are fundamentally built upon

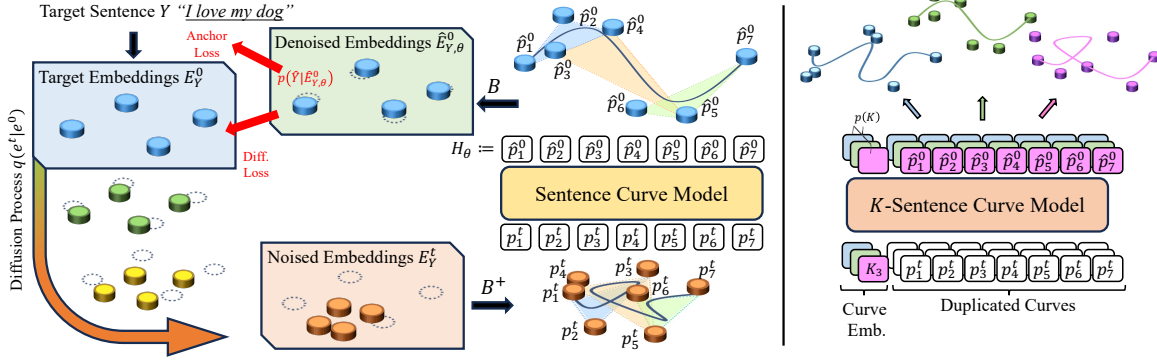


Figure 2. (Left) Overview of our SCLM’s training process at noising step t (Section 4.2). Starting from ‘Target Sentence’ and its ‘Target Embeddings’, noise is added to obtain ‘Noised Embeddings’. Then, it is mapped to sentence curve (noised), $[\mathbf{p}_i^t]_{i=1}^L$, and fed into the model. The model predicts a denoised sentence curve $[\hat{\mathbf{p}}_i^0]_{i=1}^L$, which is mapped back to ‘Denoised Embeddings’ for loss computation. (Right) Illustration of the K -sentence curve prediction scheme.

a non-AR decoding scheme and therefore vulnerable to the multimodality problem. Although extensive iterative refinement and KD act as partial mitigations, prior work has shown that DLMs still require additional remedies to fully address this issue (Wu et al., 2023; Feng et al., 2025).

2.3. Diffusion Language Models

Following the success of diffusion generative models in the image domain (Ho et al., 2020), diffusion-based approaches have been actively explored for text generation, leading to DLMs. A diffusion model consists of a forward (diffusion) process that gradually adds noise to data and a reverse (denoising) process that removes this noise. Depending on whether these processes operate in continuous or discrete spaces, DLMs can be categorized into Gaussian (continuous) DLMs and discrete DLMs. Below, we briefly review Gaussian DLMs and contrast them with discrete DLMs.

In Gaussian DLMs, a discrete target sentence Y is first mapped into a continuous embedding sequence $E_Y = [\mathbf{e}_y]_{i=1}^L$, which is treated as clean latent variables $[\mathbf{e}_i^0]_{i=1}^L$. The forward and reverse processes on a latent variable $\mathbf{e}^0 \in [\mathbf{e}_i^0]_{i=1}^L$ are defined as

$$q(\mathbf{e}^t | \mathbf{e}^0) = \mathcal{N} \left(\mathbf{e}^t; \sqrt{\alpha^t} \mathbf{e}^0, (1 - \bar{\alpha}^t) \mathbf{I}_d \right),$$

$$p_\theta(\mathbf{e}^{t-1} | \mathbf{e}^t) = \mathcal{N} \left(\mathbf{e}^{t-1}; \mu_\theta(\mathbf{e}^t, t), (1 - \alpha^t) \mathbf{I}_d \right).$$

Here, \mathbf{e}^t denotes the latent variable at diffusion step $t \in \{1, \dots, T\}$, α^t is a predefined noise schedule, and $\bar{\alpha}^t = \prod_{i=1}^t \alpha^i$. $\mathcal{N}(\cdot; \mu, \Sigma)$ denotes the Gaussian distribution that has μ mean and Σ covariance parameters. \mathbf{I}_d is $d \times d$ identity matrix. Most Gaussian DLMs adopt an efficient parameterization in which the reverse model directly predicts the clean latent variable $\hat{\mathbf{e}}_\theta^0(\mathbf{e}^t, t) := \frac{1}{\sqrt{\bar{\alpha}^t}} \mu_\theta(\mathbf{e}^t, t)$. Training is performed by minimizing the following objective:

$$\mathcal{L}_g(y; \theta, E) = \mathbb{E}_{t, \mathbf{e}^t} [\|\mathbf{e}^0 - \hat{\mathbf{e}}_\theta^0\|^2] - \log p(y | E^\top \hat{\mathbf{e}}_\theta^0). \quad (1)$$

The first term (diffusion loss) encourages accurate reconstruction of the clean embedding, while the second term (anchor loss) aligns the predicted continuous latent variable with discrete word targets. Note that the reverse process is globally conditioned on the input X .

In contrast, discrete DLMs operate directly in the discrete word space, treating the target sentence as clean categorical latent variables $Y^0 := Y$. Both forward and reverse processes are modeled using categorical distributions, and training minimizes a negative evidence lower bound. For MDLMs (Sahoo et al., 2024), this objective simplifies to a noise-scaled cross-entropy (CE) loss:

$$\mathcal{L}_m(y; \theta, W) = -\mathbb{E}_{t, y^t} \left[\frac{\alpha^t}{1 - \alpha^t} \log p_\theta(\hat{y}^0 = y | y^t, t) \right],$$

$$p_\theta(\hat{y}^0 | y^t, t) = \text{softmax}(W^\top \mathbf{h}_\theta(y^t, t)), \quad (2)$$

where $W \in \mathbb{R}^{d \times |\mathcal{V}|}$ denotes the projection (“logit”) matrix and $\mathbf{h}_\theta(y^t, t)$ is the hidden state produced by the backbone sequence model (e.g., Transformer). We refer readers to (Sahoo et al., 2024) for further details.

3. Static Word Embedding Prediction

In this section, we clarify our perspective on the target representation used in LMs and DLMs. Specifically, we view that *the backbone model parameterized by θ is trained to predict the embedding vector of the target word*. In Gaussian DLMs, the training objective in Eq. 1 explicitly enforces the backbone output $\hat{\mathbf{e}}_\theta^0$ to match \mathbf{e}^0 , which corresponds to the embedding vector of the target word \mathbf{e}_y .

In discrete DLMs, a similar interpretation arises if we regard the weight matrix of the logit layer, W in Eq. 2, as an embedding matrix assigned to target words. Under this view, the CE loss encourages the backbone output \mathbf{h}_θ to align with the embedding of the target word in W in order to

maximize likelihood. This connection becomes particularly clear when the input embedding matrix and the logit layer share parameters, i.e., $E = W$. For simplicity, throughout the remainder of this paper, we denote the target word embedding as e_y and assume parameter sharing for intuitive understanding, although this assumption is not necessary.

We now formalize this viewpoint by deriving a lemma that characterizes when the target word embedding becomes the optimal solution of the backbone output $H_\theta = [h_{\theta,1}, \dots, h_{\theta,L}]$ under the following generic maximum likelihood estimation (MLE) pipeline:

Definition 3.1 (Generic MLE Pipeline).

$$H_\theta \rightarrow E^\top H_\theta \rightarrow \text{softmax} \rightarrow \min_\theta CE.$$

This pipeline corresponds to a standard logistic regression-based classification procedure: (1) computing backbone’s outputs H_θ from an input, (2) projecting the outputs to logits with weight E , $E^\top H_\theta$, (3) applying softmax to obtain likelihoods, and (4) optimizing with cross-entropy (CE) loss. Such a pipeline is ubiquitous in neural classifiers, including standard LMs and discrete DLMs. Based on this pipeline and mild assumptions—including unit-norm constraints on e_y and h_θ , and local isotropy of word embeddings projected onto the tangent space at e_y —we obtain following lemma:

Lemma 3.2 (The Optimal Solution of Maximum Likelihood Estimation). *Given Assumptions A.1 and A.2, regardless of conditioning on X , $h = e_y$ is the optimal solution of MLE:*

$$E_Y = \arg \min E_{p_{\text{data}}(Y|X)}[-\log p_\theta(Y|X)].$$

The proof is provided in Appendix A.3. Based on this lemma, we interpret most LMs, including DLMs, as training their backbone models to predict the target sentence’s embedding sequence. Because these target embeddings are static with respect to neighboring words¹, this framework can encourage overfitting to word-level local structure rather than sentence-level global structure. When the input context is noisy, as in non-AR settings, this tendency may be further amplified, exacerbating the multimodality problem by favoring accurate single-word predictions without sufficient coordination across target words.

4. Sentence Curve

In this section, we introduce sentence curves, our core idea motivated by the probabilistic curves for time-series data (Hug et al., 2020). We first formally define the sentence curve, then apply sentence curve prediction to DLMs, resulting in sentence curve language models (Figure 2). Finally, we explain how sentence curve prediction encourages

¹Here, “static” does not indicate that embeddings or logit weights are frozen during training.

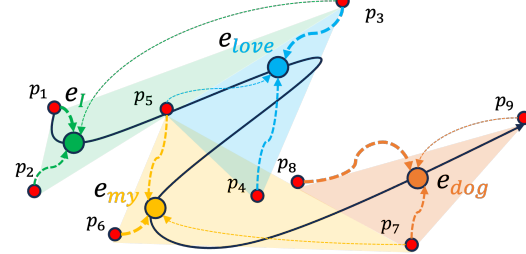


Figure 3. Illustration of control points and embeddings for the sentence “I love my dog” with $\eta = 3$. Smaller red dots denote control points (\mathbf{p}), and larger dots denote word embeddings (\mathbf{e}). The black curve represents the spline generated by the control points, while colored dotted lines indicate each control point’s contribution to embeddings, weighted by $b_{\eta,j}$. Colored triangles show the convex hulls formed by contributing control point groups.

sentence-level global structure modeling while mitigating overfitting to word-level local structure.

4.1. Definition of Sentence Curve

For the construction of sentence curves, we adapt the B-spline curve function. A B-spline curve is defined as

$$\mathbf{z}(\gamma) = \sum_{j=1}^N b_\eta(\gamma)_j \mathbf{p}_j \in \mathbb{R}^d,$$

where $P = [\mathbf{p}_j]_{j=1}^N \in \mathbb{R}^{d \times N}$ denotes the set of control points that determine the curve shape in d -dimensional space, and N is the number of control points. The basis function $b_\eta(\gamma) \in [0, 1]^N$, satisfying $\sum b_\eta(\gamma) = 1$, is a B-spline basis of degree η , which controls how many neighboring control points contribute to each curve segment. As a result, each curve segment lies within the convex hull of its contributing control points. The parameter γ denotes the curve index at which $\mathbf{z}(\gamma)$ is evaluated.

Given a sentence of length L , we sample L points from the curve at predefined indices $\Gamma = (\gamma_1, \dots, \gamma_L)$, yielding $Z_\Gamma = [\mathbf{z}(\gamma_1), \dots, \mathbf{z}(\gamma_L)] \in \mathbb{R}^{d \times L}$. We define these sampled points to be the embedding sequence of the sentence, i.e., $E_Y = Z_\Gamma$. Let $B_{\Gamma,\eta} := [b_\eta(\gamma_1), \dots, b_\eta(\gamma_L)] \in [0, 1]^{N \times L}$. Then, the relationship between the embedding sequence and the control points is given by

$$E_Y = P_Y B_{\Gamma,\eta}, \quad (3)$$

where $B_{\Gamma,\eta}$ serves as a linear mapping from control points P_Y to embeddings E_Y . This mapping process is illustrated in Figure 3. We refer to P_Y as the *sentence curve* of Y . Importantly, each control point contributes to multiple word embeddings with different weights. Consequently, modifying a single word embedding affects multiple control points simultaneously, implying that control points may encode information shared across multiple words and thus capture contextual, sentence-level structure.

In addition to the forward mapping $P \rightarrow E$, we also define an approximate inverse mapping $E \rightarrow P$, which is required for applying sentence curves to DLMs and for later theoretical analysis. Since $B_{\Gamma, \eta} \in [0, 1]^{N \times L}$ is generally non-invertible when $N \neq L$, we instead use its pseudo-inverse $B^+ := (B^\top B)^{-1} B^\top \in \mathbb{R}^{L \times N}$ as an approximation. This yields the approximation $P_Y \approx E_Y B^+$. For brevity, we omit Γ and η symbols. We refer readers to Appendix C.2 for an analysis of the reliability and information loss of the B and B^+ mappings under different hyperparameter choices, including L , N , and η . This analysis suggests that choosing $N > L$ is preferable to minimize information loss.

4.2. Sentence Curve Language Models

Based on the definition of sentence curves (Section 4.1), we propose a modified maximum likelihood estimation pipeline, termed sentence curve prediction:

Definition 4.1 (Sentence Curve Prediction).

$$H_\theta \rightarrow H_\theta B \rightarrow E^\top (H_\theta B) \rightarrow \text{softmax} \rightarrow \min_\theta CE.$$

This pipeline introduces an additional linear mapping from H_θ to $H_\theta B$, which then serves as the final hidden representation in place of H_θ in the original MLE pipeline (Definition 3.1). By Lemma 3.2, the optimal solution of $H_\theta B$ corresponds to the target embedding sequence $E_Y = P_Y B$. Accordingly, the optimal solution of H_θ can be interpreted as a set of control points P_Y that satisfies Eq. 3. As a result, sentence curve prediction trains the backbone model to predict the sentence curve of the target sentence, rather than the conventional sequence of static word embeddings.

We next describe how sentence curve prediction is incorporated into DLMs (Section 2.3) to construct SCLMs. Our description focuses on Gaussian DLMs, though the same procedure applies to discrete DLMs. Given a clean embedded target sentence E_Y^0 and its t -step noised version E_Y^t , we first apply the inverse mapping $E \rightarrow P$ using a predefined B^+ to obtain the noised sentence curve P_Y^t . The reverse process backbone then takes P_Y^t as input and produces $H_\theta(P_Y^t, t)$. Applying the forward mapping $P \rightarrow E$ with B yields the denoised embedding sequence $\hat{E}_{Y, \theta}^0$, which is used to compute the diffusion and anchor losses in Eq. 1. The whole process is illustrated in Figure 2. Overall, SCLM introduces two sentence-curve mappings—one at the input and one at the output of the backbone model. The same idea extends naturally to discrete DLMs (e.g., MDLMs) by applying $E \rightarrow P$ to the backbone’s input embeddings and $P \rightarrow E$ to its outputs before the logit projection. At testing time, that is generation from pure noise, the same input–output modifications are applied consistently.

While sentence curve prediction may encourage global structure modeling, a single predicted curve can collapse multiple

modes when the target distribution is multimodal, yielding an averaged sentence curve. To address this, we propose K -sentence curve prediction, which jointly predicts K candidate sentence curves. Specifically, we duplicate the input sentence curve as expanded batch samples and prepend a learnable curve-specific embedding tokens. The model outputs K sentence curves, whose curve embedding representations are processed by a shallow neural network to estimate their probabilities (Figure 2, right). During training, we compute a probability-weighted combination of the K curves, while at inference we select the most probable one.

4.3. Theoretic Studies of Sentence Curve Prediction

In this section, we theoretically analyze how sentence curve prediction regularizes the backbone model to emphasize sentence-level global structure, thereby mitigating overfitting to word-level local structure, as discussed in the introduction. We derive the MLE objective under sentence curve prediction, summarized by the following lemma:

Lemma 4.2 (MLE Objective in Sentence Curve Prediction (Simplified)). *Based on the setting in Section 4.1, the MLE objective can be expressed as*

$$CE_Y = CE_P - \mathbb{E}_Y [KL(P|Y, X)] + \mathcal{C}, \quad (4)$$

where \mathcal{C} denotes terms constant with respect to θ , and $KL(\cdot)$ is the Kullback-Leibler (KL) divergence.

The full derivation of this lemma are provided in Appendix A.3. During training, minimizing the standard objective $CE_Y = \mathbb{E}_{p_{\text{data}}(Y|X)}[-\log p_\theta(Y|X)]$ implicitly promotes minimization of $CE_P = \mathbb{E}_{p_{\text{data}}(P|X)}[-\log p_\theta(P|X)]$. Therefore, SCLM is encouraged to assign high likelihood to valid sentence curves that map to the target sentence via B . Because each control point influences multiple words, this objective may increase sensitivity to sentence-level global structure.

A notable thing is that multiple sentence curves can correspond to the same target sentence. Specifically, the set of valid sentence curves for a given Y forms a fiber set $\mathcal{F}_Y = \{P | PB = E_Y\}$. The model should determine which sentence curve within this fiber set to select. The internal posterior induced by the second (KL) term in Eq. 4, $p(P|Y, X)$, represents the probability of a sentence curve P given the observed Y and conditioning X . This can be interpreted as additional supervision over specific fibers, beyond what is inferred from X alone. Maximizing this KL term regularizes the model against strictly following fine-grained, dataset-specific supervision. In practice, the true data distribution over fibers is unknown and difficult to estimate. Our use of an approximate inverse mapping based on B^+ (Section 4.1) effectively selects a representative fiber, but may bias the model toward a single, easily recoverable sentence curve, potentially limiting diversity. In this setting,

Table 1. SacreBLEU (\uparrow) results on the IWSLT14 and WMT14 benchmarks. Among DLMs, the best results are shown in **bold** and the second-best are underlined. Scores without superscripts are taken directly from the original papers, except for Transformer and Diffomer, which are evaluated by us. Superscripts $*/\dagger/\ddagger/\S$ indicate results reported in prior work (Ye et al., 2023a)/(Gao et al., 2024)/(Wu et al., 2023)/(Arriola et al., 2025).

Model	IWSLT14 En→De	IWSLT14 De→En	WMT14 En→De	WMT14 De→En
Transformer (beam=1)	27.19	32.89	26.57	30.72
Transformer (beam=5)	28.24	33.83	27.71	32.00
<i>DLM baselines</i>				
DiffusionLM (Li et al., 2022) [*]	-	29.11	17.41	-
CDCD (Dieleman et al., 2022) [†]	-	-	19.7	25.4
SeqDiffuSeq (Yuan et al., 2022)	22.12	30.45	19.76	23.93
DINOISER (Ye et al., 2023b)	26.14	31.61	25.88	<u>30.30</u>
GENIE (Lin et al., 2023) [‡]	23.89	29.45	-	-
AR-Diffusion (Wu et al., 2023)	26.01	31.80	-	-
RDM (Zheng et al., 2023) [*]	-	32.14	26.54	-
MDLM (Sahoo et al., 2024) [§]	-	-	18.4	-
Diffomer (Gao et al., 2024) w/o KD	22.99	28.58	-	-
Diffomer (Gao et al., 2024) w/ KD	<u>27.21</u>	31.19	<u>27.13</u>	30.02
WDR (Heo et al., 2024)	26.26	31.83	-	-
E2D2 (Arriola et al., 2025)	-	-	24.8	-
NeoDiff (Li et al., 2025)	-	<u>32.20</u>	24.64	-
SCLM (ours) w/o KD	26.10	31.21	-	-
SCLM (ours) w/ KD	27.52	32.56	27.78	30.96

the KL term can act as a beneficial regularizer, discouraging collapse to a single fiber and helping preserve generalization across diverse sentence curve predictions.

Next, we characterize the type of global structure emphasized by SCLMs and quantify the breadth of this emphasis. The following lemma summarizes this analysis:

Lemma 4.3. *Let the model error be $V := E_Y - \hat{E}_{Y,\theta} \in \mathbb{R}^{d \times L}$ and $p_\theta(P|X) = \mathcal{N}(P; \hat{P}_\theta, \sigma^2 \mathbf{I}_d)$. Then,*

$$CE_P(V) \propto \|B^+V\|^2. \quad (5)$$

Defining the error importance as $I(V) = \|B^+V\|^2$, the relative importance of global versus local errors is given by

$$R(B^+) = \frac{I(V_{\text{global}})}{I(V_{\text{local}})} \leq \frac{\lambda_{\max}}{\lambda_{\min}}, \quad (6)$$

where λ denotes the eigenvalue of $B^+(B^+)^T$, and $V_{\text{global}} = \mathbf{1}_{d \times L} / \sqrt{dL}$, $V_{\text{local},i} = \mathbf{1}_d \delta_i^T$ represent global and local (i -th position) errors, respectively.

Eq. 5 shows that the contribution of an error V to the objective is determined by its alignment with B^+ . Consequently, SCLMs emphasize error directions that are consistent with the structure imposed by the sentence curve mapping. The smoothness property of the B-spline basis therefore encourage coherent, sentence-level error patterns. Moreover, Eq. 6 provides a quantitative measure of this effect: when B^+ exhibits a small number of dominant eigenvalues, global errors receive substantially higher importance than local ones. In contrast, if the eigenvalues of B^+ are more uniform, the

distinction between global and local error importance diminishes. As a limiting case, when B^+ is the identity matrix (i.e., $\lambda_{\max}/\lambda_{\min} = 1$), SCLM reduces to a conventional language model with no preference on global structure.

5. Experiments and Results

Our experiments consist of two parts: primary experiments on DLMs and additional experiments on semi-AR language modeling. In the DLM setting, we demonstrate the practical advantages of SCLMs on NMT, with a particular focus on their performance improvements and robustness. We also investigate the potential of SCLMs for language modeling comparing with MDLM. In the semi-AR experimental setting, we conduct qualitative analyses showing that SCLMs induce stronger correlations among final word logits than conventional word embedding prediction, consistent with the theoretical analysis in Section 4.3.

5.1. Dataset

For DLM-based NMT experiments, we use IWSLT14 En→De (Cettolo et al., 2014) and WMT14 En→De (Bojar et al., 2014) datasets, following common practice in prior DLM studies. We produced KD dataset for IWSLT14 by our AR Transformer model, and we adopt the publicly available KD dataset for WMT14 (Gao et al., 2024). For language modeling experiments with MDLM, we use the LM1B dataset (Chelba et al., 2013). Finally, for semi-AR experiments, we use WikiText-2 (Merity et al., 2016). We provide dataset-related details in Appendix B.1.

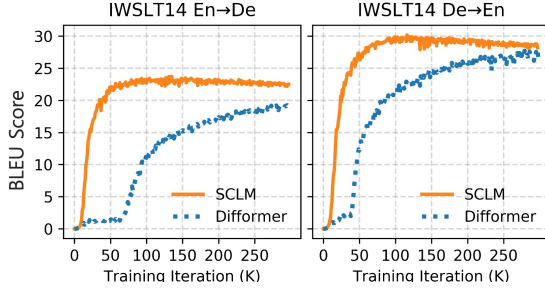


Figure 4. Validation graphs of Diffomer and SCLM without KD. To ensure sufficient convergence, Diffomer is trained for 500K iterations, and the resulting test scores are reported in Table 1.

5.2. Implementation and Configurations

Our proposed SCLMs introduce several tunable hyperparameters, including the number of control points N , sentence curve degree η , and the number of predicted sentence curves K . We set $N = \text{trunc}(LN_{ratio})$ to adapt to sentence length L , and control η either via $\eta = \max(\text{trunc}(N\eta_{ratio}), 2)$ or by fixing $\eta = \eta_{fix}$. Curve sampling indices Γ are defined as L uniformly spaced points in $[0 + m, , 1 - m]$, with margin $m = 0.01$. Given these settings, the matrices B and B^+ are determined; to reduce training overhead, we pre-computed them for all configurations and sentence lengths $L \in 2, \dots, 250$.

For DLM experiments, we build SCLMs on top of Diffomer (Gao et al., 2024) and MDLM (Sahoo et al., 2024), which are widely adopted baselines for conditional text generation and language modeling. Detailed configurations and validation-selected hyperparameters are provided in Appendix B.2, with the tuning process summarized in Table 6. SCLMs introduce no additional parameters in most settings, except for marginal overhead in K -sentence curve variants. For semi-AR experiments, we use a Transformer–LSTM hybrid for N -gram language modeling, where the Transformer decoder initializes the hidden state of the LSTM that generates N -gram words. Further architectural and hyperparameter details are provided in Appendix B.3.

5.3. DLM Experiment Results

For evaluating NMT performance, we use SacreBLEU (Post, 2018)² to ensure fair and reproducible comparisons on the IWSLT14 and WMT14 benchmarks. We report SacreBLEU scores from prior DLM studies evaluated on the same datasets; Transformer and Diffomer are evaluated under our environmental setting. Table 1 compares our SCLMs with previous methods. Notably, ‘SCLM w/ KD’ achieves SOTA scores across all benchmarks. Compared to our development baseline, Diffomer, ‘SCLM w/ KD’ improves performance by 0.31/1.37 on IWSLT14 En→De/De→En and 0.65/0.94

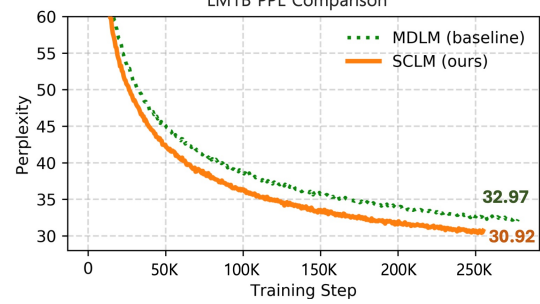


Figure 5. Evaluation PPL (↓) trends of MDLM and our SCLM during training.

on WMT14 En→De/De→En, respectively. Moreover, it matches the performance of the AR Transformer baseline on WMT14 En→De.

Surprisingly, ‘SCLM w/o KD’ achieves competitive performance compared to prior methods, while significantly outperforming its direct counterpart, ‘Diffomer w/o KD’. In addition to higher final performance, SCLMs also exhibit faster convergence than Diffomers, as shown in Figure 4. We attribute this behavior to the inherent robustness of SCLMs in global structure modeling, which mitigates the multimodality problem and reduces their reliance on KD.

Next, we compare SCLM with MDLM on the LM1B language modeling benchmark. Figure 5 shows the perplexity (PPL) trends on the evaluation set during training. We observe that SCLM consistently achieves lower perplexity than MDLM from early training stages, indicating its strong potential for language modeling. These results suggest that, beyond NMT, SCLM can be effectively applied to a broad range of tasks.

5.4. Semi-AR Experiment Results

With the WikiText-2 dataset, we conduct semi-AR language modeling experiments with a Transformer–LSTM architecture. We vary the prediction horizon from 3-gram to 5-gram. For each setting, performance is evaluated using the average PPL, defined as $\frac{1}{N} \sum_{n=1}^N PPL_n$. Across 3-/4-/5-gram prediction tasks, the baseline model with conventional word embedding prediction achieves average PPLs of **295.33** / **366.14** / **420.32**, respectively, while SCLMs consistently obtain better PPLs of **287.75** / **358.37** / **411.89**.

Under this setting, we empirically analyze SCLM’s global structure enforcement using distance correlation (Székely et al., 2007). After injecting dropout and Gaussian noise into the Transformer’s final hidden state, we measure distance correlations between the resulting logit vectors across N -gram predictions. Noise is scaled by the hidden-state norm to control for scale differences. As shown in Figure 6, SCLMs consistently yield higher correlations than baselines,

²Signature:BLEU+case.mixed+numrefs.1+smooth.exp+tok.13a+version.1.5.1

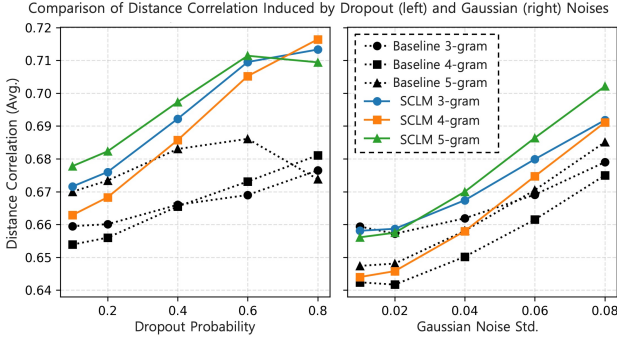


Figure 6. Distance correlation analysis with baselines and SCLMs.

supporting our theoretical claim that they better model the sentence-level global structure.

6. Related Works and Discussions

6.1. Curves in Machine Learning

Spline curve functions (e.g., Bézier curves and B-splines) have been adopted across several machine learning domains. In computer vision, curve-based representations have been integrated into neural networks for tasks such as graph and 3D meshing (Fey et al., 2018), and lane detection (Feng et al., 2022). These works leverage the geometric properties of curves as inductive priors tailored to their respective tasks. Similarly, our sentence curve can be considered as an inductive prior of sentence’s latent structure.

Our approach is most closely related to Hug et al. (Hug et al., 2020), which apply Bézier curves to multi-step time-series prediction. While inspired by this direction, our work differs in several key aspects. First, we adopt the more general B-spline formulation, enabling flexible control over the strength and type of regularization. Second, we explicitly handle the inverse mapping via a pseudo-inverse construction, allowing seamless integration with DLMs. Moreover, to the best of our knowledge, this work is the first to bridge sentences and spline curves in the language modeling domain. Unlike continuous signals, sentences are abstract and symbolic, exhibiting complex latent structure; nevertheless, our results demonstrate that neural models can discover meaningful curve representations even in high-dimensional word embedding spaces.

6.2. Sentence Target Diversification and Why Curves?

To our knowledge, few prior works explore alternative target sentence representations. Word difference representations (WDRs) were proposed to diversify the representation of target sentence considering neighbor words (Heo et al., 2024). While this approach improves performance and gradient diversity, it remains auxiliary to conventional word embedding prediction and follows a multi-task learning paradigm. In

contrast, our sentence curve prediction fully replaces word-level targets with a curve-based representation, yielding stronger performance improvements.

There is extensive body of prior work on the compositionality of word embeddings (Xu et al., 2015; Hartung et al., 2017; Poliak et al., 2017; Scheepers et al., 2018; Li et al., 2018; Frandsen & Ge, 2019). In addition, large neural encoders such as BERT (Devlin et al., 2019) and modern large language models provide powerful contextualized representations that achieve strong performance across a wide range of downstream tasks. However, these representations are almost exclusively used on the input side of models, whereas our focus is on the target side.

Designing alternative target representations imposes stricter requirements. First and most importantly, the representation must be decodable, meaning it can be mapped back to the original sequence of discrete words. If contextualization compresses or entangles information irreversibly, it becomes unsuitable as a target. Second, the decoding process must be computationally simple. Although large decoders for BERT or LLMs could, in principle, enable decodability, their use as target decoders would be impractical due to the high computational cost of backpropagation. For these reasons, we argue that sentence curves provide an effective and practical alternative target representation for sentences.

7. Conclusion and Discussion

In this paper, we propose sentence curves, a curve-based continuous representation of sentences, as an alternative to conventional word embeddings. By using sentence curves as target representations, we develop sentence curve language models (SCLMs). We theoretically argue that sentence curve prediction encourages modeling of contextual, sentence-level global structure, and our extensive experiments demonstrate consistent performance improvements in neural machine translation and language modeling. Furthermore, our empirical analyses provide strong evidence supporting the theoretical motivations behind SCLMs.

As an initial exploration of this direction, our work has several limitations that suggest avenues for future research. In particular, due to the number of control points exceeding the sentence length, the computational cost of the backbone model substantially increases. In our experiments, SCLMs require several times longer training and inference times than baseline models (Table 4 in Appendix B.2). While this work focuses on demonstrating the feasibility and benefits of sentence curve prediction, future research may substantially mitigate this overhead, for example by deriving control points from intermediate hidden states rather than processing them directly at the input layer. We leave such efficiency improvements to future work.

References

Achiam, J., Adler, S., Agarwal, S., Ahmad, L., Akkaya, I., Aleman, F. L., Almeida, D., Altenschmidt, J., Altman, S., Anadkat, S., et al. Gpt-4 technical report. *arXiv preprint arXiv:2303.08774*, 2023.

Arora, S., Li, Y., Liang, Y., Ma, T., and Risteski, A. A latent variable model approach to pmi-based word embeddings. *Transactions of the Association for Computational Linguistics*, 4:385–399, 2016.

Arriola, M., Schiff, Y., Phung, H., Gokaslan, A., and Kuleshov, V. Encoder-decoder diffusion language models for efficient training and inference. *arXiv preprint arXiv:2510.22852*, 2025.

Bojar, O., Buck, C., Federmann, C., Haddow, B., Koehn, P., Leveling, J., Monz, C., Pecina, P., Post, M., Saint-Amand, H., et al. Findings of the 2014 workshop on statistical machine translation. In *Proceedings of the ninth workshop on statistical machine translation*, pp. 12–58, 2014.

Cai, T., Li, Y., Geng, Z., Peng, H., Lee, J. D., Chen, D., and Dao, T. Medusa: Simple llm inference acceleration framework with multiple decoding heads. *arXiv preprint arXiv:2401.10774*, 2024.

Cettolo, M., Niehues, J., Stüker, S., Bentivogli, L., and Federico, M. Report on the 11th iwslt evaluation campaign. In *Proceedings of the 11th International Workshop on Spoken Language Translation: Evaluation Campaign*, pp. 2–17, 2014.

Chelba, C., Mikolov, T., Schuster, M., Ge, Q., Brants, T., Koehn, P., and Robinson, T. One billion word benchmark for measuring progress in statistical language modeling. *arXiv preprint arXiv:1312.3005*, 2013.

Devlin, J., Chang, M.-W., Lee, K., and Toutanova, K. Bert: Pre-training of deep bidirectional transformers for language understanding. In *Proceedings of the 2019 conference of the North American chapter of the association for computational linguistics: human language technologies, volume 1 (long and short papers)*, pp. 4171–4186, 2019.

Dieleman, S., Sartran, L., Roshannai, A., Savinov, N., Ganin, Y., Richemond, P. H., Doucet, A., Strudel, R., Dyer, C., Durkan, C., et al. Continuous diffusion for categorical data. *arXiv preprint arXiv:2211.15089*, 2022.

Feng, G., Geng, Y., Guan, J., Wu, W., Wang, L., and He, D. Theoretical benefit and limitation of diffusion language model. *arXiv preprint arXiv:2502.09622*, 2025.

Feng, Z., Guo, S., Tan, X., Xu, K., Wang, M., and Ma, L. Rethinking efficient lane detection via curve modeling. In *Proceedings of the IEEE/CVF conference on computer vision and pattern recognition*, pp. 17062–17070, 2022.

Fey, M., Lenssen, J. E., Weichert, F., and Müller, H. Splinecnn: Fast geometric deep learning with continuous b-spline kernels. In *Proceedings of the IEEE conference on computer vision and pattern recognition*, pp. 869–877, 2018.

Frandsen, A. and Ge, R. Understanding composition of word embeddings via tensor decomposition. *arXiv preprint arXiv:1902.00613*, 2019.

Gao, Z., Guo, J., Tan, X., Zhu, Y., Zhang, F., Bian, J., and Xu, L. Empowering diffusion models on the embedding space for text generation. In *Proceedings of the 2024 Conference of the North American Chapter of the Association for Computational Linguistics: Human Language Technologies (Volume 1: Long Papers)*, pp. 4664–4683, 2024.

Gemini, Anil, R., Borgeaud, S., Alayrac, J.-B., Yu, J., Soricut, R., Schalkwyk, J., Dai, A. M., Hauth, A., Millican, K., et al. Gemini: a family of highly capable multimodal models. *arXiv preprint arXiv:2312.11805*, 2023.

Gloewkler, F., Idrissi, B. Y., Rozière, B., Lopez-Paz, D., and Synnaeve, G. Better & faster large language models via multi-token prediction. *arXiv preprint arXiv:2404.19737*, 2024.

Gu, J., Bradbury, J., Xiong, C., Li, V. O., and Socher, R. Non-autoregressive neural machine translation. *arXiv preprint arXiv:1711.02281*, 2017.

Hartung, M., Kaupmann, F., Jebbara, S., and Cimiano, P. Learning compositionality functions on word embeddings for modelling attribute meaning in adjective-noun phrases. In *Proceedings of the 15th Conference of the European Chapter of the Association for Computational Linguistics: Volume 1, Long Papers*, pp. 54–64, 2017.

Heo, D. and Choi, H. Shared latent space by both languages in non-autoregressive neural machine translation. *arXiv preprint arXiv:2305.03511*, 2023.

Heo, D., Rim, D. N., and Choi, H. N-gram prediction and word difference representations for language modeling. *arXiv preprint arXiv:2409.03295*, 2024.

Ho, J., Jain, A., and Abbeel, P. Denoising diffusion probabilistic models. *Advances in neural information processing systems*, 33:6840–6851, 2020.

Huang, F., Tao, T., Zhou, H., Li, L., and Huang, M. On the learning of non-autoregressive transformers. In *International conference on machine learning*, pp. 9356–9376. PMLR, 2022.

Hug, R., Hübner, W., and Arens, M. Introducing probabilistic bézier curves for n-step sequence prediction. In *Proceedings of the AAAI Conference on Artificial Intelligence*, volume 34, pp. 10162–10169, 2020.

Ildiz, M. E., Huang, Y., Li, Y., Rawat, A. S., and Oymak, S. From self-attention to markov models: Unveiling the dynamics of generative transformers. *arXiv preprint arXiv:2402.13512*, 2024.

Jang, E., Gu, S., and Poole, B. Categorical reparameterization with gumbel-softmax. *arXiv preprint arXiv:1611.01144*, 2016.

Kim, Y. and Rush, A. M. Sequence-level knowledge distillation. In *Proceedings of the 2016 conference on empirical methods in natural language processing*, pp. 1317–1327, 2016.

Lee, J., Mansimov, E., and Cho, K. Deterministic non-autoregressive neural sequence modeling by iterative refinement. *arXiv preprint arXiv:1802.06901*, 2018.

Li, B., Drozd, A., Liu, T., and Du, X. Subword-level composition functions for learning word embeddings. In *Proceedings of the second workshop on subword/character level models*, pp. 38–48, 2018.

Li, B., Gao, Z., and Xu, L. Unifying continuous and discrete text diffusion with non-simultaneous diffusion processes. *arXiv preprint arXiv:2505.22165*, 2025.

Li, X., Thickstun, J., Gulrajani, I., Liang, P. S., and Hashimoto, T. B. Diffusion-lm improves controllable text generation. *Advances in neural information processing systems*, 35:4328–4343, 2022.

Lin, Z., Gong, Y., Shen, Y., Wu, T., Fan, Z., Lin, C., Duan, N., and Chen, W. Text generation with diffusion language models: A pre-training approach with continuous paragraph denoise. In *International Conference on Machine Learning*, pp. 21051–21064. PMLR, 2023.

Liu, J., Zhai, Y., and Chen, Z. Normalization of input-output shared embeddings in text generation models. *arXiv preprint arXiv:2001.07885*, 2020.

Meng, Y., Huang, J., Wang, G., Zhang, C., Zhuang, H., Kaplan, L., and Han, J. Spherical text embedding. *Advances in neural information processing systems*, 32, 2019.

Merity, S., Xiong, C., Bradbury, J., and Socher, R. Pointer sentinel mixture models. *arXiv preprint arXiv:1609.07843*, 2016.

Mikolov, T., Sutskever, I., Chen, K., Corrado, G. S., and Dean, J. Distributed representations of words and phrases and their compositionality. *Advances in neural information processing systems*, 26, 2013.

Nie, S., Zhu, F., You, Z., Zhang, X., Ou, J., Hu, J., Zhou, J., Lin, Y., Wen, J.-R., and Li, C. Large language diffusion models. *arXiv preprint arXiv:2502.09992*, 2025.

Ott, M., Edunov, S., Baevski, A., Fan, A., Gross, S., Ng, N., Grangier, D., and Auli, M. fairseq: A fast, extensible toolkit for sequence modeling. *arXiv preprint arXiv:1904.01038*, 2019.

Peebles, W. and Xie, S. Scalable diffusion models with transformers. In *Proceedings of the IEEE/CVF international conference on computer vision*, pp. 4195–4205, 2023.

Poliak, A., Rastogi, P., Martin, M. P., and Van Durme, B. Efficient, compositional, order-sensitive n-gram embeddings. In *Proceedings of the 15th Conference of the European Chapter of the Association for Computational Linguistics: Volume 2, Short Papers*, pp. 503–508, 2017.

Post, M. A call for clarity in reporting BLEU scores. In *Proceedings of the Third Conference on Machine Translation: Research Papers*, pp. 186–191, Belgium, Brussels, October 2018. Association for Computational Linguistics. URL <https://www.aclweb.org/anthology/W18-6319>.

Sahoo, S., Arriola, M., Schiff, Y., Gokaslan, A., Marroquin, E., Chiu, J., Rush, A., and Kuleshov, V. Simple and effective masked diffusion language models. *Advances in Neural Information Processing Systems*, 37:130136–130184, 2024.

Scheepers, T., Kanoulas, E., and Gavves, E. Improving word embedding compositionality using lexicographic definitions. In *Proceedings of the 2018 World Wide Web Conference*, pp. 1083–1093, 2018.

Shu, R., Lee, J., Nakayama, H., and Cho, K. Latent-variable non-autoregressive neural machine translation with deterministic inference using a delta posterior. In *Proceedings of the aaai conference on artificial intelligence*, volume 34, pp. 8846–8853, 2020.

Székely, G. J., Rizzo, M. L., and Bakirov, N. K. Measuring and testing dependence by correlation of distances. 2007.

Vaswani, A., Shazeer, N., Parmar, N., Uszkoreit, J., Jones, L., Gomez, A. N., Kaiser, Ł., and Polosukhin, I. Attention is all you need. *Advances in neural information processing systems*, 30, 2017.

Wu, T., Fan, Z., Liu, X., Zheng, H.-T., Gong, Y., Jiao, J., Li, J., Guo, J., Duan, N., Chen, W., et al. Ar-diffusion: Auto-regressive diffusion model for text generation. *Advances in Neural Information Processing Systems*, 36:39957–39974, 2023.

Xu, R., Chen, T., Xia, Y., Lu, Q., Liu, B., and Wang, X.

Word embedding composition for data imbalances in sentiment and emotion classification. *Cognitive Computation*, 7:226–240, 2015.

Ye, J., Zheng, Z., Bao, Y., Qian, L., and Gu, Q. Diffusion language models can perform many tasks with scaling and instruction-finetuning. *arXiv preprint arXiv:2308.12219*, 2023a.

Ye, J., Zheng, Z., Bao, Y., Qian, L., and Wang, M. Dinoiser: Diffused conditional sequence learning by manipulating noises. *arXiv preprint arXiv:2302.10025*, 2023b.

Yuan, H., Yuan, Z., Tan, C., Huang, F., and Huang, S. Seqdiffuseq: Text diffusion with encoder-decoder transformers. *arXiv preprint arXiv:2212.10325*, 2022.

Zheng, L., Yuan, J., Yu, L., and Kong, L. A reparameterized discrete diffusion model for text generation. *arXiv preprint arXiv:2302.05737*, 2023.

A. Mathematic Backgrounds

A.1. Assumptions

Assumption A.1 (Unit Norm Constraint).

$$\|\mathbf{e}_i\|^2 = \|\mathbf{h}\|^2 = 1 \quad \forall i \in \{1, \dots, |\mathcal{V}|\}.$$

This assumption constrains all embedding vectors and the backbone output to lie on the unit sphere \mathbb{S}^{d-1} , allowing the analysis to focus on vector orientations rather than trivial scale differences. This normalization has also been shown to be practically effective in prior work (Meng et al., 2019; Liu et al., 2020).

Assumption A.2 (Local Isotropy (Arora et al., 2016) on the Target Embedding's Tangent Space). Given a target word y ,

$$\mathbb{E}[\mathbf{u}_i] = 0, \quad \mathbf{u}_i = \mathbf{e}_i - (\mathbf{e}_y^\top \mathbf{e}_i) \mathbf{e}_y \quad \forall i \in \{1, \dots, |\mathcal{V}|\}.$$

This assumption states that, conditioned on a target word y , the remaining word embeddings are isotropically distributed when projected onto the tangent space of \mathbf{e}_y . Although this assumption may appear strong, it is considerably weaker than commonly adopted alternatives such as orthonormal logit bases (Ildiz et al., 2024), which require $d \geq |\mathcal{V}|$ and impose rigid structural constraints. In contrast, our assumption permits $d < |\mathcal{V}|$, as well as semantic similarity and clustered embedding structures.

A.2. Structural Equivalence of Continuous Relaxation and General MLE Pipeline

In this section, we explain the connection between the word and its embedding in the context of continuous relaxation (Jang et al., 2016). In continuous relaxation, the embedding vector can be regarded as the mean of approximated word in the continuous space. Our next proposition says the details:

Proposition A.3 (Continuous Relaxation of Words). *With defining $\mathbf{z}_y = E\delta_y + \epsilon$ where $\epsilon \sim \mathcal{N}(\mathbf{0}, \sigma^2 \mathbf{I}_d)$,*

$$\begin{aligned} p(\mathbf{z}_y|y) &= \mathcal{N}(\mathbf{e}_y, \sigma^2 \mathbf{I}), \\ p(y|\mathbf{z}_y) &= \text{softmax}(E^\top \mathbf{z}_y / \sigma^2), \end{aligned}$$

conditioned on Assumption A.1 and when $E^\top : \mathbb{R}^{|\mathcal{V}|} \rightarrow \mathbb{R}^d$ is injective.

Proof. The likelihood distribution, $p(\mathbf{z}_y|y)$ is determined by the definition. By Bayes theorem,

$$p(y|\mathbf{z}_y) = \frac{p(\mathbf{z}_y|y)p(y)}{\sum_{k=1}^{|\mathcal{V}|} p(\mathbf{z}_y|y=k)p(y=k)} = \frac{p(y)e^{-\frac{1}{2\sigma^2} \|\mathbf{z}_y - \mathbf{e}_y\|^2}}{\sum_{k=1}^{|\mathcal{V}|} p(y=k)e^{-\frac{1}{2\sigma^2} \|\mathbf{z}_y - \mathbf{e}_k\|^2}}.$$

Based on Assumption A.1, $\|\mathbf{z}_y - \mathbf{e}_k\|^2 = 2 - 2\mathbf{e}_k^\top \mathbf{z}$. With plugging this into the above formulation:

$$\begin{aligned} p(y|\mathbf{z}_y) &\approx \frac{p(y)e^{(\mathbf{e}_y^\top \mathbf{z}_y - 1)/\sigma^2}}{\sum_{k=1}^{|\mathcal{V}|} p(y=k)e^{(\mathbf{e}_k^\top \mathbf{z}_y - 1)/\sigma^2}} = \frac{p(y)e^{\mathbf{e}_y^\top \mathbf{z}_y / \sigma^2}}{\sum_{k=1}^{|\mathcal{V}|} p(y=k)e^{\mathbf{e}_k^\top \mathbf{z}_y / \sigma^2}} \\ &\approx \frac{e^{\mathbf{e}_y^\top \mathbf{z}_y / \sigma^2}}{\sum_{k=1}^{|\mathcal{V}|} e^{\mathbf{e}_k^\top \mathbf{z}_y / \sigma^2}} = \text{softmax}(E^\top \mathbf{z}_y / \sigma^2), \end{aligned}$$

with assuming $p(y=k) \quad \forall k \in \{1, \dots, |\mathcal{V}|\}$ is constant. \square

In other words, \mathbf{z}_y is an approximation of the word y in d -dimensional continuous space, and the embedding vector \mathbf{e}_y is the mean of \mathbf{z}_y . Interestingly, the likelihood distribution, $p(y|\mathbf{z}_y)$ has similar form with the generic MLE pipeline (Definition 3.1 in Section 3). With switching \mathbf{z}_y to \mathbf{h} , and assuming $\sigma^2 = 1$, the likelihood has structural equivalence between the pipeline's likelihood estimation process. In this sense, what the model is trying to do can be understood as predicting a latent variable \mathbf{z} in the continuous space that is aligned to the word y with mapping E and E^\top .

A.3. Proofs of Theorems and Lemmas

Lemma A.4 (The Optimal Solution of Maximum Likelihood Estimation). *Given Assumptions A.1 and A.2, regardless of conditioning on X , $\mathbf{h} = \mathbf{e}_y$ is the optimal solution of MLE:*

$$E_Y = \arg \min_{H_\theta} \mathbb{E}_{p_{data}(Y|X)} [-\log p_\theta(Y|X)].$$

Proof. Without loss of generality, we focus on the minimization of a target word $y \in Y$: $\arg \min_{\mathbf{h}} -\log p(y|X)$, note that we omitted θ for brevity.

To derive the optimal solution given the condition $\|\mathbf{h}\|^2 = 1$ (Assumption A.1), we use Lagrange multiplier. In result, the objective function can be derived follows:

$$\begin{aligned} L(\mathbf{h}, \lambda) &= f(\mathbf{h}) - \lambda(\|\mathbf{h}\|^2 - 1), \\ \nabla_{\mathbf{h}} L(\mathbf{h}, \lambda) &= \nabla_{\mathbf{h}} f(\mathbf{h}) - 2\lambda \mathbf{h}, \end{aligned}$$

where $f(\mathbf{h}) = -\log p(y|X) = \mathbf{e}_y^\top \mathbf{h} - \log \sum_k e^{\mathbf{e}_k^\top \mathbf{h}}$ by the general pipeline (Section 3 and Appendix A.2). Based on this formulation, the stationary condition of Lagrange multiplier becomes:

$$\nabla f(\mathbf{h}) = 2\lambda \mathbf{h}.$$

Notably, this informs that $\nabla_{\mathbf{h}} f(\mathbf{h})$ is a parallel vector to \mathbf{h} , in turn, the tangent component of $\nabla_{\mathbf{h}} f(\mathbf{h})$ with respect to \mathbf{h} should be zero. This is formulated as follows:

$$\nabla_{\mathbf{h}} f(\mathbf{h}) - (\mathbf{h}^\top \nabla_{\mathbf{h}} f(\mathbf{h})) \mathbf{h} = 0.$$

With plugging the formulation of $f(\mathbf{h})$ into the above, the stationary condition becomes:

$$\mathbf{e}_y - \sum_k p(y=k|\mathbf{h}) \mathbf{e}_k - \left(\mathbf{h}^\top \mathbf{e}_k - \mathbf{h}^\top \left(\sum_k p(y=k|\mathbf{h}) \mathbf{e}_y \right) \mathbf{e}_y \right) \mathbf{h} = 0. \quad (7)$$

Now, to verify our main conjecture which is the optimality of $\mathbf{e}_y = \mathbf{h}$, we set $\mathbf{h}^* = \mathbf{e}_y$ in Eq. 7, and validate whether the condition holds or not. After plugging our conjecture, the stationary condition is derived as follows:

$$\begin{aligned} \sum_k p(y=k|\mathbf{e}_y) (\mathbf{e}_k - (\mathbf{e}_y^\top \mathbf{e}_k) \mathbf{e}_y) &= \sum_{k, k \neq y} p(y=k|\mathbf{e}_y) (\mathbf{e}_k - (\mathbf{e}_y^\top \mathbf{e}_k) \mathbf{e}_y) \\ &= \mathbb{E}_{p(y=k|\mathbf{e}_y)} [\mathbf{e}_k] - \mathbb{E}_{p(y=k|\mathbf{e}_y)} [(\mathbf{e}_y^\top \mathbf{e}_k) \mathbf{e}_y] = 0. \end{aligned} \quad (8)$$

Given the target embedding \mathbf{e}_y , all the other embedding vector can be decomposed into parallel and tangent components with respect to \mathbf{e}_y : $\mathbf{e}_i = (\mathbf{e}_y^\top \mathbf{e}_i) \mathbf{e}_y + (\mathbf{e}_i - (\mathbf{e}_y^\top \mathbf{e}_i) \mathbf{e}_y)$. We denote the tangent component as $\mathbf{u}_i = \mathbf{e}_i - (\mathbf{e}_y^\top \mathbf{e}_i) \mathbf{e}_y$. Based on this decomposition and the given assumption (Assumption A.2), the expectation term becomes:

$$\mathbb{E}[\mathbf{e}_k] = \mathbb{E}[(\mathbf{e}_y^\top \mathbf{e}_k) \mathbf{e}_y + \mathbf{u}_k] = \mathbb{E}[(\mathbf{e}_y^\top \mathbf{e}_k) \mathbf{e}_y].$$

This makes the stationary, Eq. 8, be satisfied. Consequently, our conjecture of the optimality $\mathbf{e}_y = \mathbf{h}$ is proved. \square

Lemma A.5 (MLE Objective in Sentence Curve Prediction). *With assuming Y and E are equal in distribution, both marginally and conditionally on any variables, such as P and X , via $\sigma^2 \rightarrow 0$ in continuous relaxation scheme (Appendix A.2). Based on settings in Section 4.1, the MLE objective function is derived as follows:*

$$CE_Y = CE_P - \mathbb{E}_Y [KL(P|Y, X)] + \mathcal{C},$$

where \mathcal{C} indicates constant terms with respect to θ . $KL(\cdot)$ is Kullback-Leibler (KL) divergence.

Proof. By Bayes theorem, the log-likelihood of Y given X is derived as follows:

$$\begin{aligned}\log p_\theta(Y|X) &= \log p_\theta(Y|P, X) + \log p_\theta(P|X) - \log p_\theta(P|Y, X) \\ &= \log p(Y|P) + \log p_\theta(P|X) - \log p_\theta(P|Y, X),\end{aligned}$$

where the second equation is done by considering $P \xrightarrow{B} Y$ is deterministic many-to-one mapping. With applying expectation over $p_{data}(Y, P|X)$, we have that:

$$\begin{aligned}\underbrace{\mathbb{E}_{p_{data}(Y|X)}[-\log p_\theta(Y|X)]}_{=CE_Y} &= \underbrace{\mathbb{E}_{p_{data}(P|X)}[-\log p_\theta(P|X)]}_{=CE_P} + \mathbb{E}_{p_{data}(Y, P|X)}[\log p_\theta(P|Y, X)] + \underbrace{\mathbb{E}_{p_{data}(Y, P|X)}[-\log p(Y|P)]}_{=\mathbb{E}_{P|X}[\mathcal{H}(Y|P)](\text{constant})} \\ &= CE_P + \mathbb{E}_{p_{data}(Y|X)} \left[\underbrace{\mathbb{E}_{p_{data}(P|Y, X)} \left[-\log \frac{p_{data}(P|Y, X)}{p_\theta(P|Y, X)} \right]}_{=-KL(P|Y, X)} \right] \\ &\quad + \underbrace{\mathbb{E}_{p_{data}(Y, P|X)}[\log p_{data}(P|Y, X)] + \mathcal{C}}_{=\mathbb{E}_{Y|X}[-\mathcal{H}(P|Y, X)](\text{constant})} \\ &= CE_P - \mathbb{E}_Y[KL(P|Y, X)] + \mathcal{C}\end{aligned}$$

□

Lemma A.6. Let the model error be $V := E_Y - \hat{E}_{Y,\theta} \in \mathbb{R}^{d \times L}$ and $p_\theta(P|X) = \mathcal{N}(P; \hat{P}_\theta, \sigma^2 \mathbf{I}_d)$ for any variance σ^2 . Then,

$$CE_P(V) \propto \|B^+V\|^2. \quad (9)$$

Defining the error importance as $I(V) = \|B^+V\|^2$, the relative importance of global versus local errors under B^+ is given by

$$R(B^+) = \frac{I(V_{global})}{I(V_{local})} \leq \frac{\lambda_{max}}{\lambda_{min}}, \quad (10)$$

where λ denotes the eigenvalue of $B^+(B^+)^T$, and $V_{global} = \mathbf{1}_{d \times L}/\sqrt{dL}$, $V_{local,i} = \mathbf{1}_d \delta_i^T$ represent global and local (i -th position) errors, respectively.

Proof. Based on the definition of the model's error in E -space, $V = E_Y - \hat{E}_{Y,\theta}$, we derive the error in P -space as $V_P : P_Y - \hat{P}_\theta = E_Y B^+ - \hat{E}_{Y,\theta} B^+ = V B^+$. From now on, we concentrate on one dimension out of d for simple derivation without loss of generality. For example, we assume $E_Y \in \mathbb{R}^L$, $P \in \mathbb{R}^N$, $V \in \mathbb{R}^L$, and $V B^+ \in \mathbb{R}^N$. The negative log-likelihood of CE_P can be derived as follows:

$$\begin{aligned}-\log p_\theta(P|X) &= \frac{1}{2\sigma^2} \|P - \hat{P}_\theta\|^2 = \frac{1}{2\sigma^2} \|V B^+\|^2, \\ CE_P &\propto \|V B^+\|^2.\end{aligned}$$

$\|V B^+\|^2 = (V B^+)(V B^+)^T$ can be further derived to $V B^+ (B^+)^T V^T$. For simplicity, we express $G = B^+ (B^+)^T \in \mathbb{R}^{L \times L}$. Because G is positive semi-definite matrix, it has an eigen-decomposition as follows:

$$G = \sum_{j=1}^L \lambda_j \mathbf{k}_j \mathbf{k}_j^T,$$

where λ and \mathbf{k} are eigenvalue and eigenvector of G , respectively. Based on those bases from G , we can decompose any error vector as follows:

$$V = \sum_{j=1}^L \alpha_j \mathbf{k}_j, \quad V G V^T = \sum_{j=1}^L \lambda_j \alpha_j^2,$$

where $\alpha_j = V^\top \mathbf{k}_j$ is the coefficient for the factor V with respect to \mathbf{k} vector. Based on those derivations, the global and local error importance are derived as follows:

$$\begin{aligned} I(V_{global}) &= \|V_{global} B^+\|^2 = \frac{1}{L} \|\mathbf{1}_{d \times L} B^+\|^2 = \frac{1}{L} \sum_{j=1}^L \lambda_j \left(\sum_{i=1}^L \mathbf{k}_{ji} \right)^2 \\ &\leq \lambda_{max} \left(\sum_{i=1}^L \mathbf{k}_{max,i} \right)^2 \leq \lambda_{max} \sum_{i=1}^L \mathbf{k}_{max,i}^2 = \lambda_{max}, \\ I(V_{local}) &= \|V_{local,i} B^+\|^2 = \sum_{j=1}^L \lambda_j \mathbf{k}_{jj}^2 \geq \lambda_{min} \sum_{j=1}^L \mathbf{k}_{min,j}^2 = \lambda_{min}, \end{aligned}$$

where the second inequality of global error importance is derived by Jensen's inequality. Finally, with plugging in those results, we can get

$$R(B^+) = \frac{I(V_{global})}{I(V_{local})} \leq \frac{\lambda_{max}}{\lambda_{min}}.$$

□

B. Experimental Details

B.1. Details of Datasets

In our NMT experiments, we use the IWSLT14 English–German and WMT14 English–German datasets. Data cleaning, tokenization, and byte-pair encoding (BPE) are performed using the Fairseq toolkit (Ott et al., 2019), closely following the preprocessing pipelines adopted in prior works (Ye et al., 2023b; Gao et al., 2024). After preprocessing, the IWSLT14 dataset contains approximately 160K/7K/7K sentence pairs for the train/validation/test splits, respectively, with a vocabulary size of 10K. The processed WMT14 dataset contains approximately 4.5M/3K/3K sentence pairs with a vocabulary size of 40K. For language modeling experiments based on the MDLM architecture, we use the LM1B dataset. All preprocessing steps follow the protocol described in (Sahoo et al., 2024). Notably, we do not employ sentence packing during data loading. After preprocessing, the dataset contains approximately 30M training sentences and 300K evaluation sentences. Lastly, for semi-AR experiments, we use the WikiText-2 dataset, following the preprocessing procedure provided in a public implementation³. The resulting dataset contains approximately 2M training tokens with a vocabulary size of about 33K.

B.2. Details of DLM Experiments

In this section, we describe the details of our development baseline models and training procedures. For the backbone architecture of Difformer, we use the `transformer_iwslt_de_en` and `transformer_wmt_en_de` configurations provided by the Fairseq toolkit for the IWSLT14 and WMT14 experiments, respectively, following Difformer's diffusion-based training framework⁴. We closely adhere to the official training scheme of Difformer for both the baseline models and our SCLMs. The full set of configuration details is summarized in Table 2. We note that our minimum Bayes risk (MBR) settings, including the length beam and noise beam sizes, are minimal or consistent with those used in prior works in Table 1. The total number of parameters for Difformer and SCLM models is 38.9M for IWSLT14 and 53.5M for WMT14, respectively. Importantly, SCLMs introduce almost no additional parameters beyond the baseline models.

For language modeling experiments with MDLM, we follow the official model implementation and training setup⁵, where the backbone architecture is DiT (Peebles & Xie, 2023). Due to computational resource constraints, we reduce the number of training iterations from default 1M to 200K, while keeping other settings unchanged. Detailed descriptions of the MDLM architecture and training protocol can be found in (Sahoo et al., 2024). Both MDLM and our SCLM variant contain approximately 139M parameters.

Finally, after hyperparameter tuning on the validation set, we select the best configurations for the SCLM components, as reported in Table 3. The explored ranges for each hyperparameter are $N_{raito} \in \{2.0, 2.5, 3.0\}$, $\eta_{raito} \in \{0.01, 0.05, 0.1, 0.2\}$,

³<https://github.com/chakki-works/chazutsu>

⁴<https://github.com/zhjgao/difformer>

⁵<https://github.com/kuleshov-group/mdlm>

Table 2. Model and training configurations for Difformer experiments.

Hyperparameter	IWSLT14 En-De	WMT14 En-De
Model / Architecture	transformer_iwslt_de_en	transformer_wmt_en_de
# Encoder layers	6	6
# Decoder layers	6	6
d_{model}	512	512
d_{ff}	1024	2048
# Attention heads	4	8
Dropout	0.3	0.1
Label smoothing	0.1	0.1
Batch size (tokens)	8K	32K
Optimizer	Adam	Adam
Learning rate schedule	Inverse sqrt + warmup	Inverse sqrt + warmup
Warmup steps	10K	4K
Learning rate	5e-4	5e-4
Gradient clipping	0.0	1.0
Training iterations	300K	300K
Checkpoint ensemble	5	5
Latent dimension	128	128
Diffusion steps	2K	2K
Rescaling factor	4.0	3.5
Self-conditioning	O	O
Reverse steps (testing)	20	20
Length Beam size (testing)	5	7
Noise Beam size (testing)	2	3

 Table 3. Tuned hyperparameters of proposed SCLM models in DLM experiments. If the value of η is float or integer, then the value is ratio or fixed value, respectively.

Hyperparameter	IWSLT14 En→De	IWSLT14 De→En	IWSLT14 En→De (w/o KD)	IWSLT14 De→En (w/o KD)	WMT14 En→De	WMT14 De→En	LM1B
N_{ratio}	2.5	3.0	2.0	2.0	2.5	2.5	0.2
η	0.1	5	0.01	0.01	0.05	0.01	0.1
K	3	1	2	3	1	1	1

$\eta_{fix} \in \{5, 10, 20\}$, and $K \in \{1, 2, 3, 4\}$.

Our experiments on WMT14 and LM1B are conducted using either an RTX 4090 or an RTX 3090 GPU. For the smaller IWSLT14 dataset, we use an A4000 GPU. We report training time and memory usage comparisons in Table 4, measured on the IWSLT14 and WMT14 datasets. Empirically, we find that the hyperparameters N_{ratio} and K are the primary factors influencing computational cost⁶. Overall, SCLMs consistently incur higher computational overhead than baseline models, primarily due to the increased number of tokens processed by the Transformer backbone.

B.3. Details for Semi-AR Experiments

In this section, we describe the implementation details of our semi-AR language models. As illustrated in Figure 7, we implement a simple architecture that predicts multiple future words in parallel. Specifically, conditioned on the final hidden state of the Transformer decoder, an additional LSTM layer predicts the embedding (or control point) vectors of future target of N-gram words (or sentence curve of N-gram). This architecture is closely related to simple N -gram prediction models proposed in prior work (Heo et al., 2024; Cai et al., 2024; Gloeckle et al., 2024), but we adopt an LSTM layer in line with the original curve-based time-series prediction framework (Hug et al., 2020). The Transformer backbone follows the configuration of a small Transformer (the `transformer_iwslt_de_en` architecture in Table 2). The additional LSTM layer is a shallow single-layer network, resulting in minimal parameter overhead. After hyperparameter tuning, we identify the optimal SCLM configurations, reported in Table 5. Interestingly, in the semi-AR setting, the optimal values of K are generally larger than those selected for the DLM experiments.

⁶Measurements for varying values of K are not yet complete; we guess larger K to further increase computational cost.

Table 4. Comparison of spending time and memory usage during training and inference. All ‘Total Inference Time (seconds)’ values are measured by 1x RTX4090 GPU.

Model	IWSLT14 En→De	IWSLT14 De→En	WMT14 En→De	WMT14 De→En
Total Training Time (hours) / Average Memory Usage (GB)				
Diffomer	19.2 / 5.8	18.8 / 5.7	22.2 / 20.4	22.3 / 20.7
SCLM ($N_{ratio} = 2.0$)	51.2 / 6.9	51.7 / 6.8	55.5 / 21.4	54.5 / 21.8
SCLM ($N_{ratio} = 2.5$)	62.3 / 7.3	54.5 / 8.6	99.0 / 23.4	98.8 / 22.9
SCLM ($N_{ratio} = 3.0$)	67.0 / 8.0	60.9 / 9.2	-	-
Total Inference Time (seconds)				
Diffomer	51.9	52.4	81.0	87.0
SCLM ($N_{ratio} = 2.0$)	495.4	497.0	464.4	521.3
SCLM ($N_{ratio} = 2.5$)	526.8	521.4	477.7	529.6
SCLM ($N_{ratio} = 3.0$)	577.8	626.9	-	-

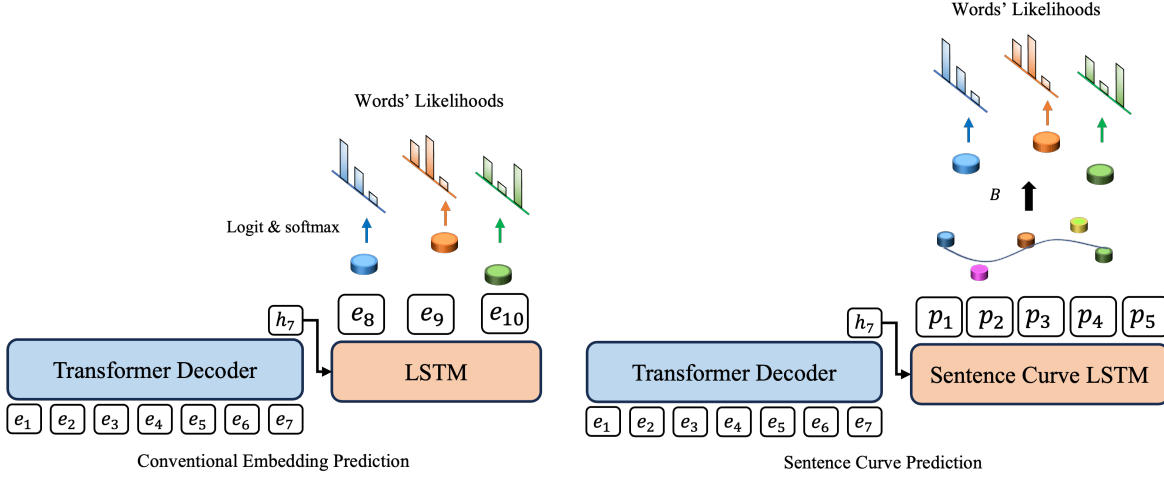


Figure 7. Semi-AR Transformer-LSTM hybrid architecture (3-gram prediction). The left panel shows the baseline model with conventional word embedding prediction, while the right panel illustrates our sentence curve prediction architecture.

C. Additional Experimental Analyses

C.1. Ablation Study on IWSLT14 De→En

In this section, we present an ablation study that illustrates our hyperparameter tuning process based on validation performance. We conducted a grid search over the predefined ranges of each hyperparameter described in Section B.2. Table 6 reports the ablation results on the IWSLT14 De→En task. As shown, we select the configuration that achieves the highest validation BLEU score. Notably, we observe consistent performance improvements over the baseline.

C.2. Information Preservation of Sentence Curve Mapping

To assess the risk of information loss in the B and B^+ mapping process, we conduct a reconstruction error analysis. Given a length- L random noise sequence sampled from a standard Gaussian distribution, we first map the sequence to the P -space using B^+ and then reconstruct it back to the original space using B . We compute the average mean squared error (MSE) between the original and reconstructed sequences. We vary the hyperparameters L , N_{ratio} , and η_{ratio} over the ranges $\{25, 50, \dots, 225, 250\}$, $\{1.0, 1.5, 2.0, 2.5, 3.0\}$, and $\{0.0, 0.33, 0.66\}$, respectively. The minimum curve degree η is fixed to 2, ensuring that at least two control points contribute to each word even when $\eta_{ratio} = 0.0$.

Figure 8 reports results averaged over 100 random noise sequences. We observe that shorter sentence lengths yield lower reconstruction errors than longer ones. In addition, increasing the number of control points reduces reconstruction error, whereas higher curve degrees η lead to larger errors. Overall, these results suggest that choosing $N_{ratio} \geq 2.0$ and $\eta_{ratio} < 0.33$ provides a safe hyperparameter regime for preserving information in short- to medium-length sentences.

Table 5. Tuned hyperparameters of proposed SCLM models for semi-AR experiments. $N = N_{fix}$ and $\eta = \eta_{fix}$ are all fixed configurations because L is fixed in semi-AR environment.

Hyperparameter	3-Gram	4-Gram	5-Gram
N_{fix}	18	20	20
η_{fix}	6	13	7
K	4	4	6

Table 6. Ablation study of the proposed SCLM model based on IWSLT14 De→En.

Model	Valid BLEU	Test BLEU
<i>Baselines</i>		
Transformer	35.71	33.83
Difformer	31.81	31.19
<i>Default Config.</i>		
SCLM ($N_{ratio} = 2.0, \eta_{ratio} = 0.1, K = 1$)	33.25	32.35
<i>Varying N_{ratio}</i>		
SCLM ($N_{ratio} = 2.0, \eta_{ratio} = 0.1, K = 1$)	33.25	32.35
SCLM ($N_{ratio} = 2.5, \eta_{ratio} = 0.1, K = 1$)	33.28	32.04
SCLM ($N_{ratio} = 3.0, \eta_{ratio} = 0.1, K = 1$)	33.63	32.41
<i>Varying η</i>		
SCLM ($N_{ratio} = 3.0, \eta_{ratio} = 0.01, K = 1$)	33.79	32.56
SCLM ($N_{ratio} = 3.0, \eta_{ratio} = 0.05, K = 1$)	33.50	32.35
SCLM ($N_{ratio} = 3.0, \eta_{ratio} = 0.1, K = 1$)	33.63	32.41
SCLM ($N_{ratio} = 3.0, \eta_{fix} = 5, K = 1$)	33.37	32.25
SCLM ($N_{ratio} = 3.0, \eta_{fix} = 10, K = 1$)	33.11	32.13
<i>Varying K</i>		
SCLM ($N_{ratio} = 3.0, \eta_{ratio} = 0.01, K = 1$)	33.79	32.56
SCLM ($N_{ratio} = 3.0, \eta_{ratio} = 0.01, K = 2$)		
SCLM ($N_{ratio} = 3.0, \eta_{ratio} = 0.01, K = 3$)		
SCLM ($N_{ratio} = 3.0, \eta_{ratio} = 0.01, K = 4$)		

C.3. Sentence Curve Generation Examples

In this section, we present additional sentence curve generation examples, analogous to the illustration in the top of Figure 1. All those examples are generated using our best-performing WMT14 De→En checkpoint. Figure 9 shows two representative sentence curve generation histories. As illustrated, SCLM smoothly denoises the sentence curve from early diffusion steps and progressively refines it toward a curve that maps to the reference sentence embeddings. Together with the examples in Figure 1 and Figure 9, all visualizations are based on the intermediate denoising variables $\hat{e}_{Y,\theta}^t$.

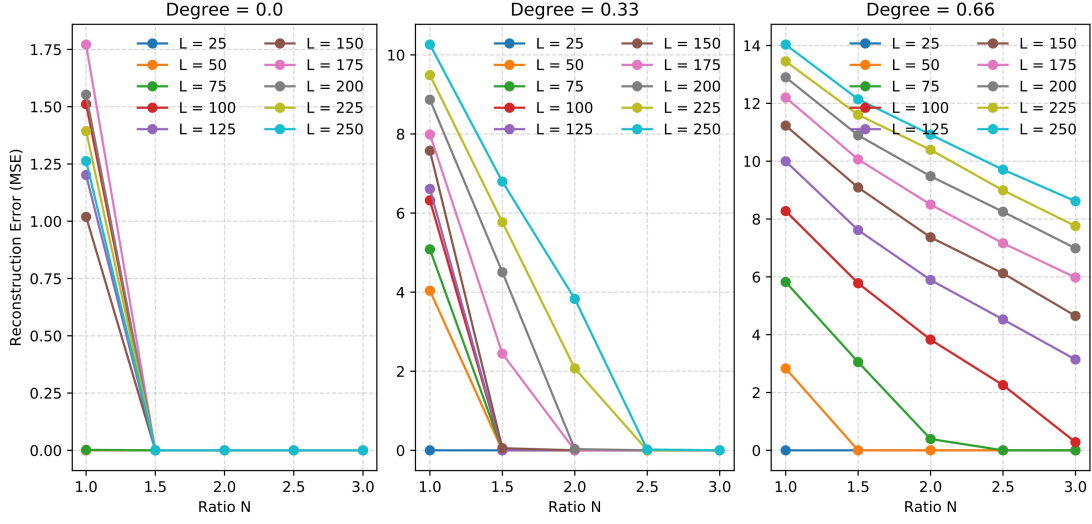
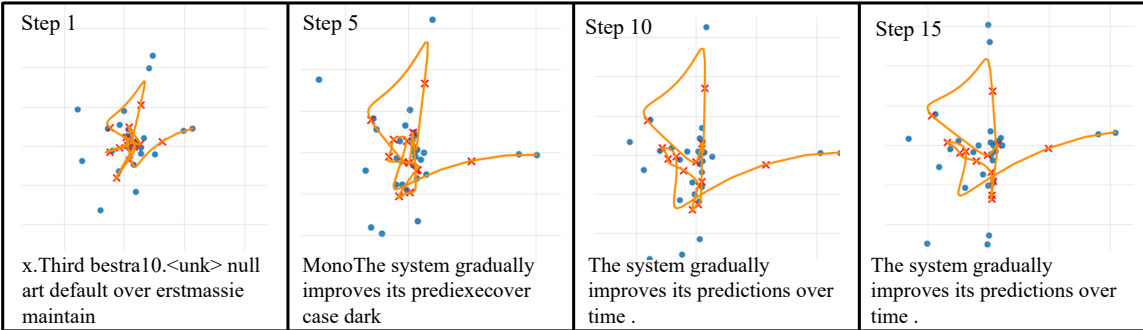


Figure 8. Reconstruction error results of sentence curve inverse mapping/mapping: $E \xrightarrow{B^+} P \xrightarrow{B} E$ process, depending on different sentence length L , N_{ratio} , and η_{ratio} .

Reference: “The system gradually improves its predictions over time.”



Reference: “Accurate results depends on careful experimental design.”

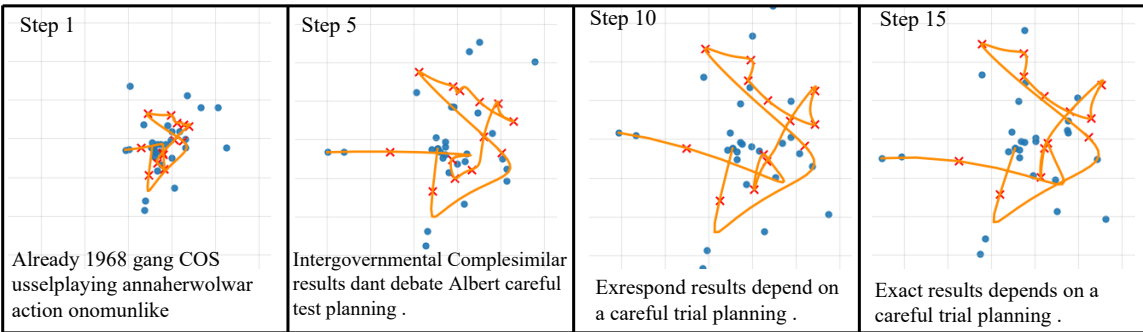


Figure 9. Extra examples of sentence curve generation based on our SCLM. Blue dots represent the estimated control points. Orange curves are the sentence curves produced from the control point sets. We marked the curve points (with red ‘X’ symbol) that are selected to be word embeddings.